Electronic Supplementary Material (ESI) for Lab on a Chip.

Supplementary Information

Rapid Isolation of Circulating Cancer Associated Fibroblasts by Acoustic Microstreaming for Assessing Metastatic Propensity of Breast Cancer Patients

Ruoyu Jiang[1], Sudhanshu Agrawal[2], Mohammad Aghaamoo[1], Ritesh Parajuli[3], Anshu Agrawal[2] & Abraham P. Lee[1,4]

[1]Biomedical Engineering, University of California, Irvine, CA 92697; [2]Department of Medicine, School of Medicine, University of California, Irvine, California; [3]Department of Medicine, Division of Hematology Oncology, University of California, Irvine, CA 92697; [4]Mechanical and Aerospace Engineering, University of California, Irvine, CA 92697

[*]E-mail: aplee@uci.edu

CONTENTS

Supplementary Video 1 caption:

Time Lapse of LCATs Blood Sample WBCs Enrichment. Scale bar: 100 μm.

Supplementary Video 2 caption:

Time-lapse of LCATs Acoustic Microstreaming Cell Capture. Scale bar: 100 μm.

Detail of Experimental Apparatus

Lateral Cavity Acoustic Transducers (LCATs) are placed on top of the piezo transducer (Steiner and Martins, Inc., USA). Ultrasonic gel is applied between the LCATs device and the piezo transducer to allow acoustic waves to propagate to the LCATs device (Fig. S1a). The piezo transducer is then connected to a 10x signal amplifier (Krohn-Hite Corp., USA) as shown in Fig. S1b. The signal amplifier is connected to a function generator (Agilent Technology, Inc., USA). The LCATs device can be controlled by frequency (1) and voltage (2) using square acoustic waves (3) as shown in Fig. S1c.

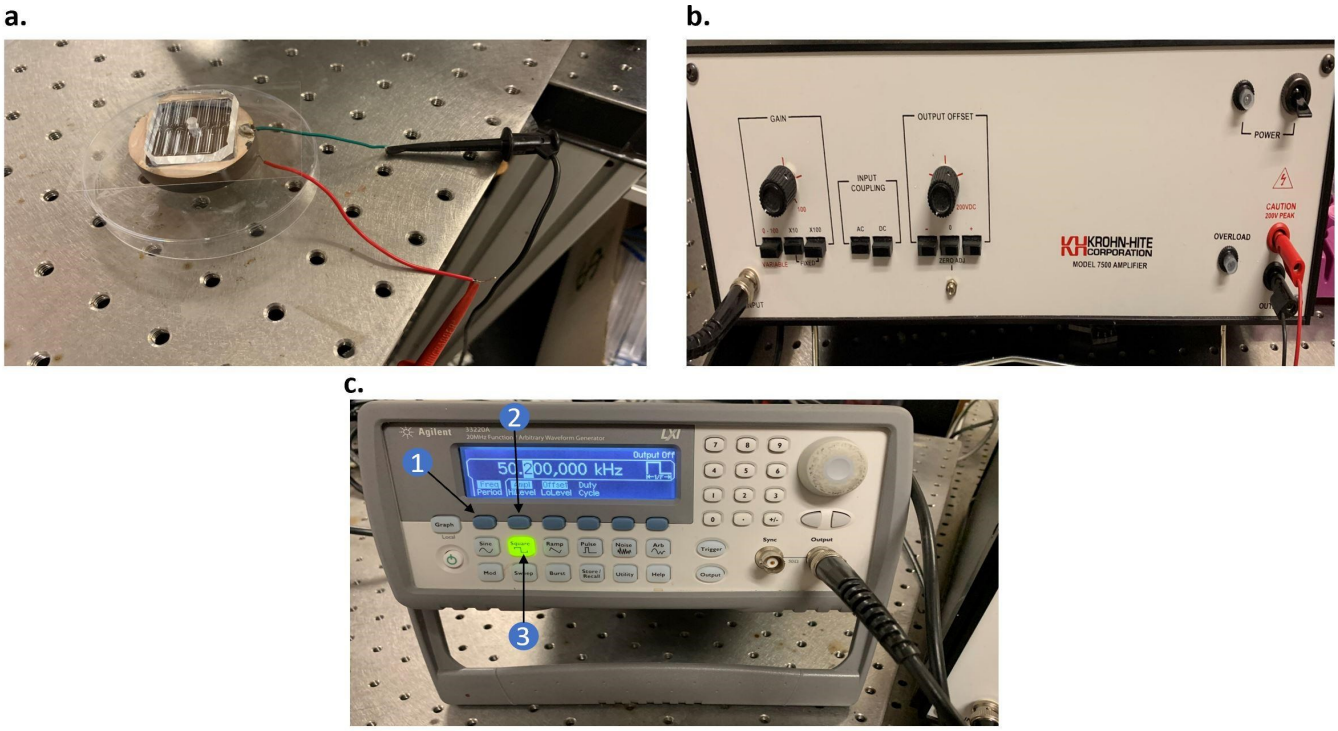

Figure S1. Equipment setup of the Lateral Cavity Acoustic Transducers (LCATs) for circulating rare cell capture. (a) The LCATs device placed on top of the piezo transducer. (b) Signal amplifier is connected to the piezo transducer and function waveform generator. (c) A function waveform generator is connected to a signal amplifier and controls frequency, voltage and type of acoustic waves.

Numerical Simulation: The Phase Field multiphase model was employed to track the interface between the air-liquid interface in the device. In addition, the Solid Mechanics module was used to simulate the oscillation of PDMS sharp tips near the lateral cavities. The two interfaces were coupled together by Fluid-Solid Interaction module. For this problem, PDMS was considered as a linear elastic materials with $E = 32\ MPa, \rho = 1070\frac{kg}{m^3},$ and $\nu = 0.495$ where E,ρ, and ν are Young's modulus, density, and Poisson's ratio, respectively. Triangular mesh elements (56000 mesh elements) were mainly used for meshing the geometries. The mesh was refined near the air-liquid interface for better accuracy.

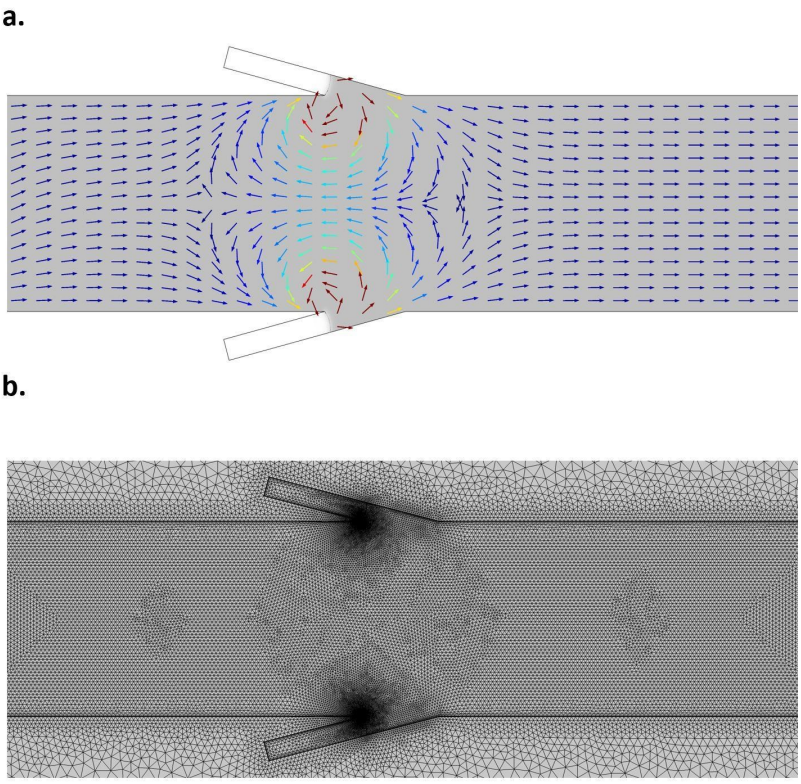

Figure S2. Numerical simulation of acoustic microstreaming at the air-liquid interface. (a) Simulation of acoustic microstreaming formation at the air-liquid interface caused by acoustic oscillation. (b) Mesh simulation of acoustic microstreaming with triangular mesh elements.

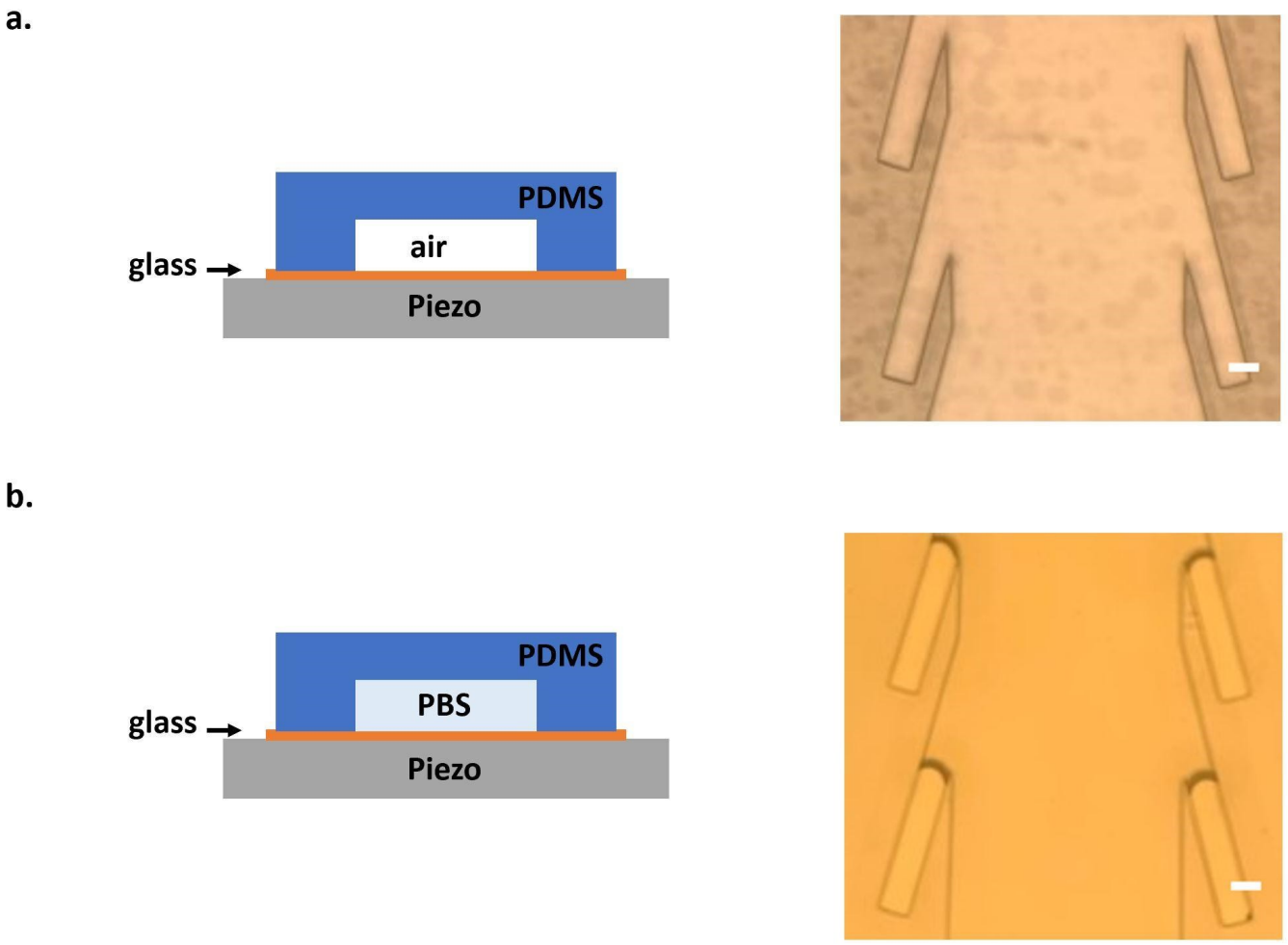

Figure S3. Microfluidic chip air-liquid interface formation. (a**)** Microfluidic chip without PBS priming. (b) Microfluidic chip with PBS priming to form air-liquid interfaces at dead-end side channels. Scale bar: 100 μm.

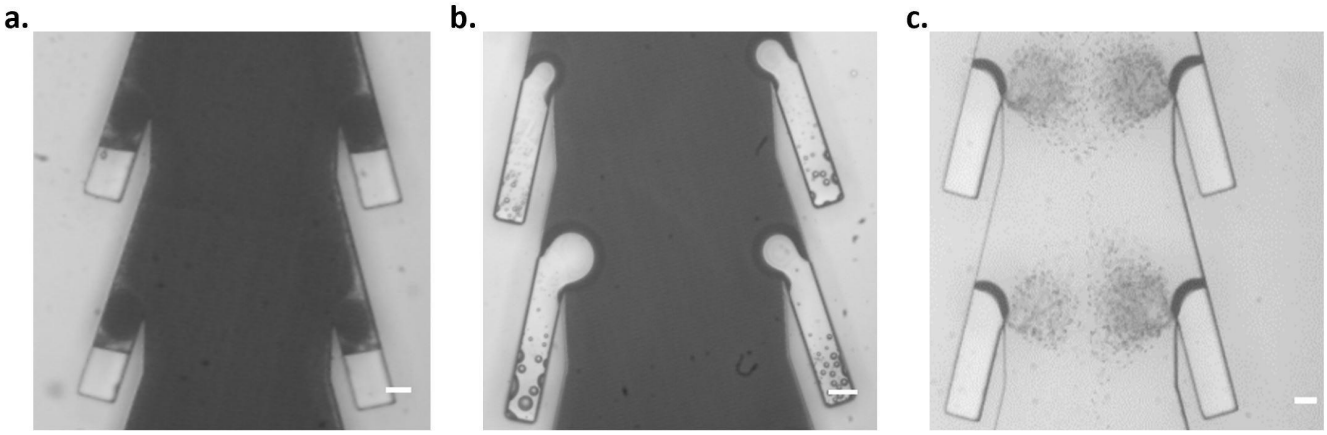

Figure S4. Stability of air-liquid interface at different sample conditions. (a) Air-liquid interface can be pushed back when pumping with an external syringe pump at 25 μL/min. (b) Air-liquid interface experiences significant deformation when the device is self-pumping whole blood at higher voltages. (c) Air-liquid interface remains stable when the device is self-pumping RBC lysed blood samples. Scale bar: 100 μm.

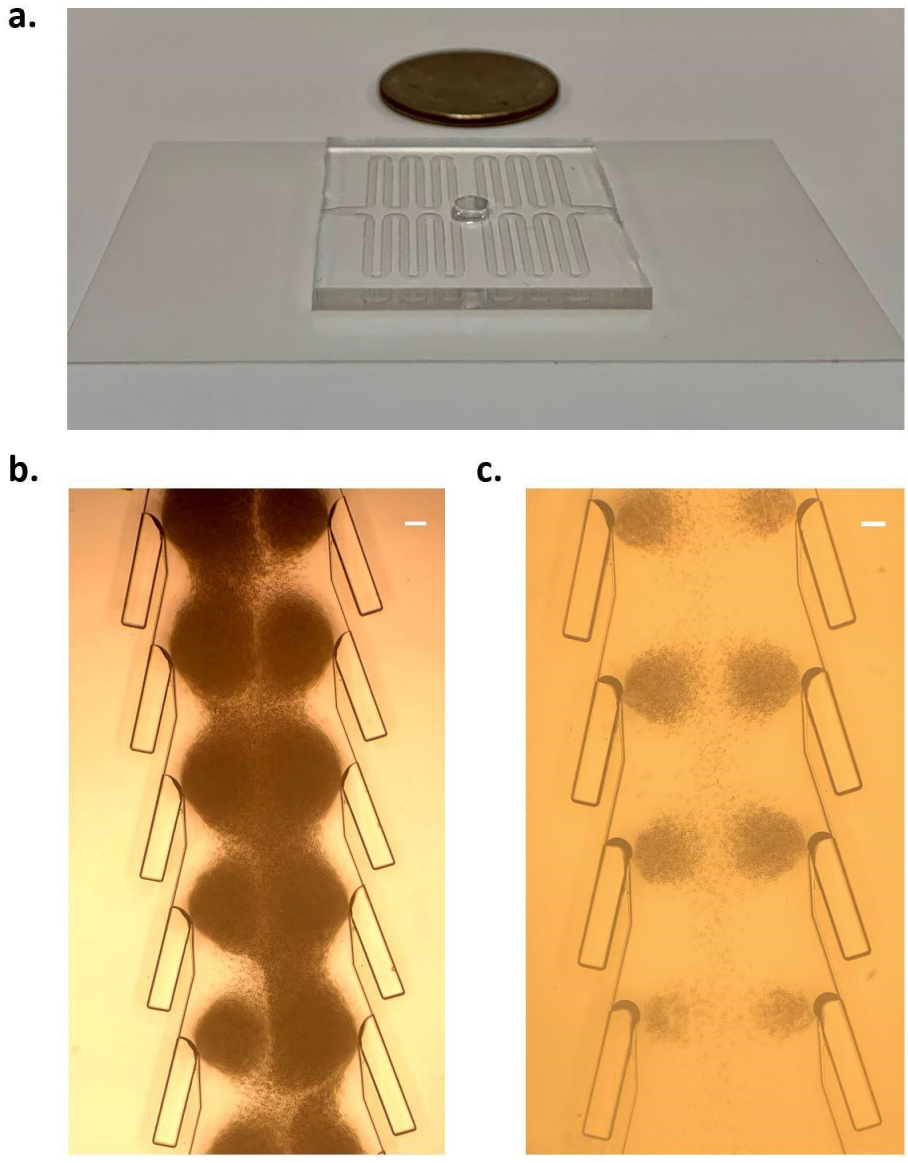

Figure S5. Lateral Cavity Acoustic Transducers (LCATs) blood processing. (a) A physical appearance of 404 pairs of LCATs chips. (b) Initial stage of LCATs with lysed blood sample. Even though most of the RBCs are lysed, there are still many RBCs remaining. (c) Acoustic microstreaming trapping of CTCs and cCAFs after washing step. Scale bar: 100 μm.

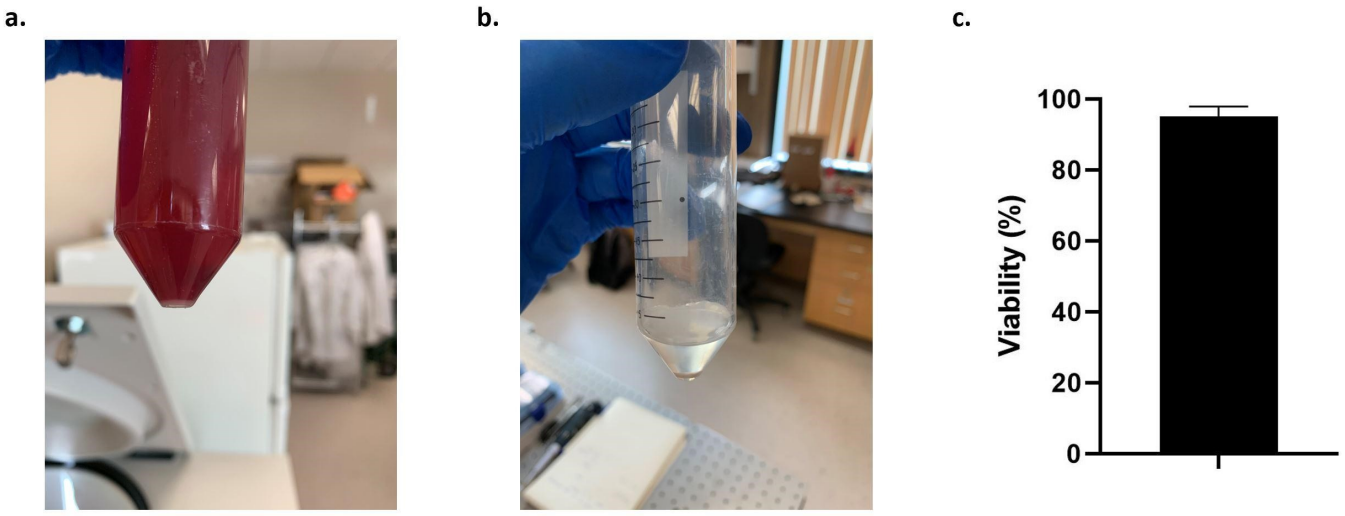

Figure S6. Whole blood pretreatment with ACK buffer. (a) Whole blood incubating with an ACK buffer and WBC cell pellets are centrifuged at the bottom. (b) RBCs are aspirated and removed, leaving WBCs. (c) Viability test from RBC lysis buffer. (N=3).

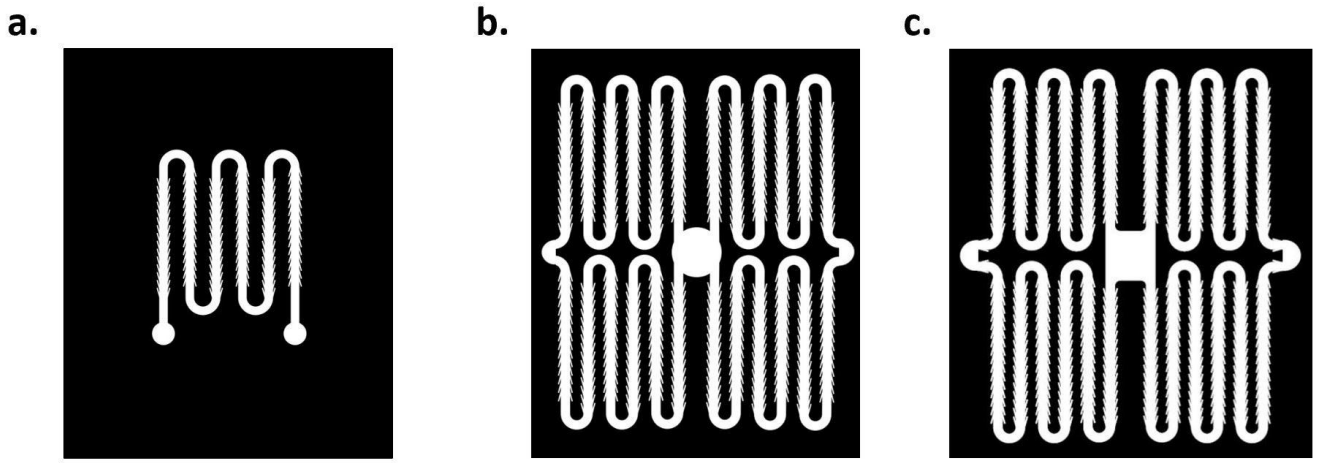

Figure S7. Plots of different configurations of LCATs devices. (a) 90 LCATs. (b) 360 LCATs. (c) 404 LCATs. (b) and (c) share the same number of columns but different number of LCATs. The increasing number of LCATs increases the pumping rate. The channel width and height of these devices are 750 μm and 100 μm.

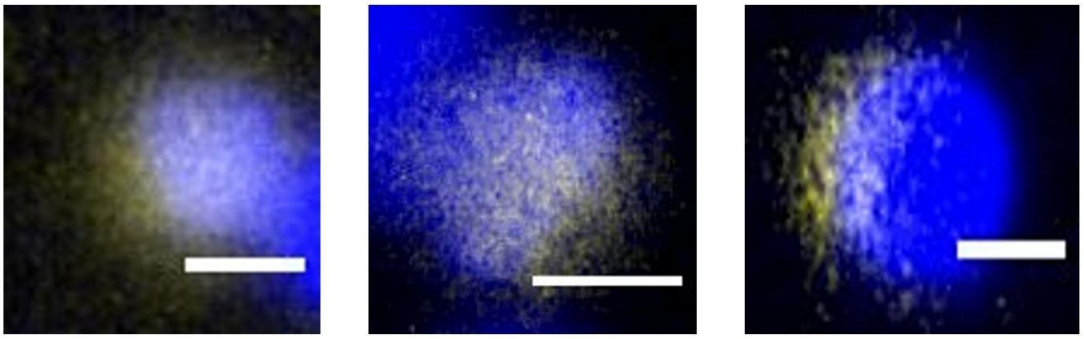

Figure S8. Fluorescent images of cCAFs being identified with α-SMA. DAPI (blue) is used to stain the cell nucleus, α-SMA is shown as yellow. Scale bar: 10 μm.

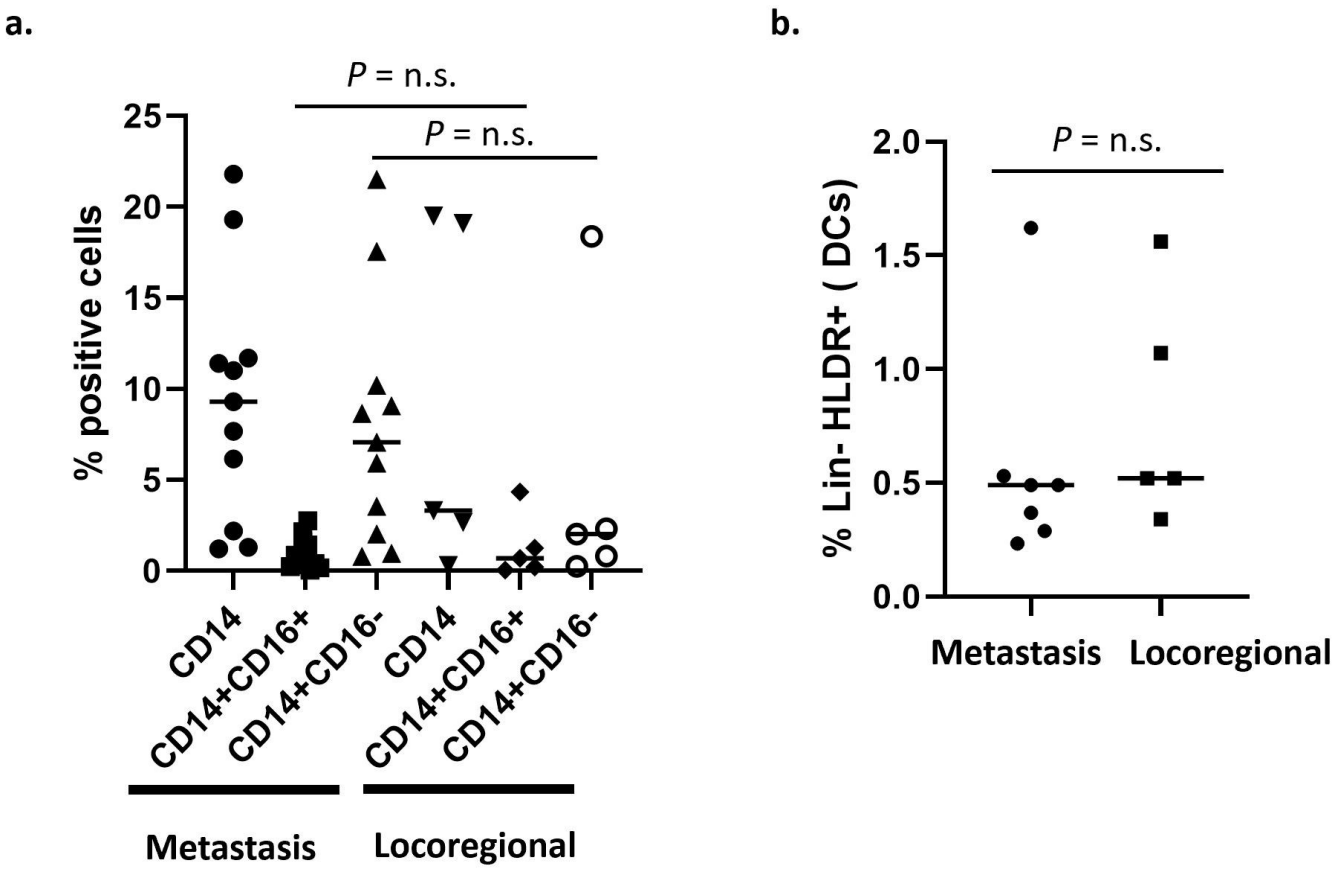

Figure S9. Cell surface marker expression level across different stages of breast cancer. (a) Innate immune cells inflammatory monocytes markers. (b) Activation markers CD86 and HLADR on blood dendritic cells. P values are non-significant.

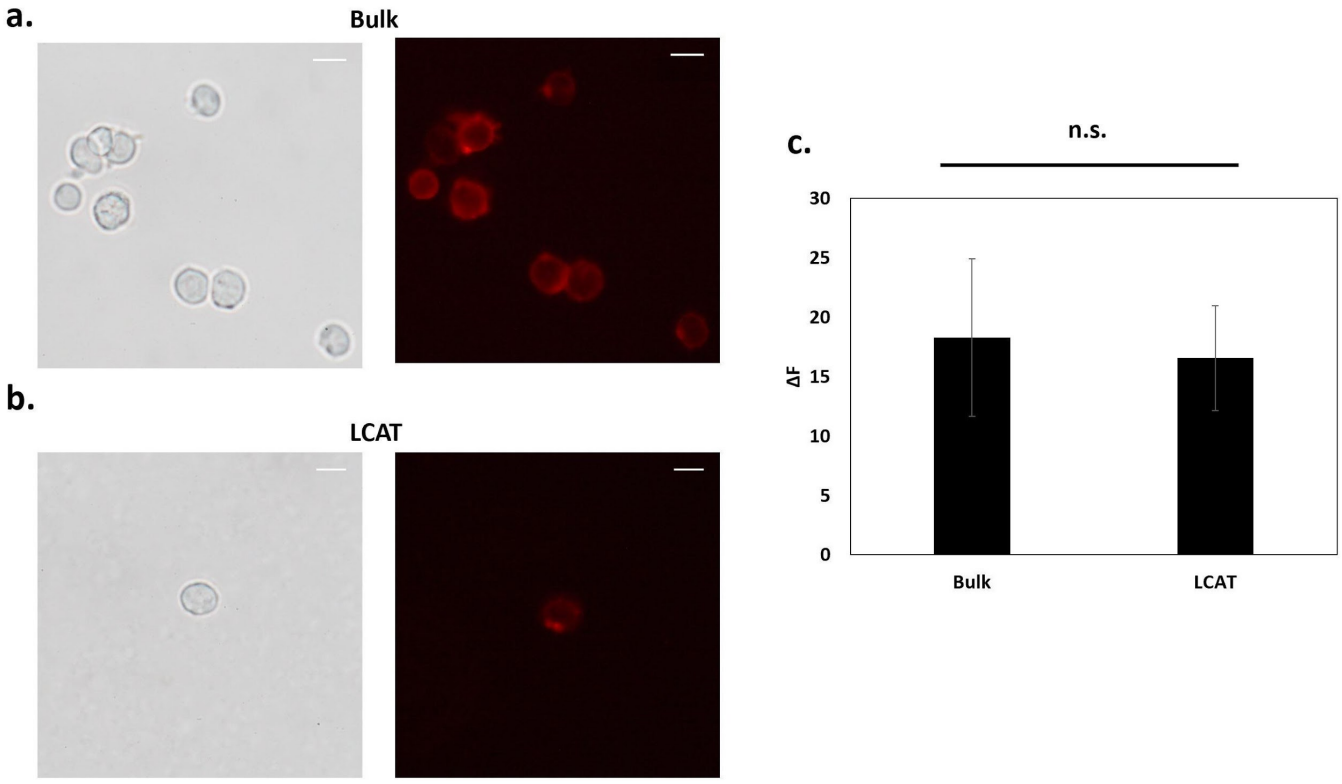

Figure S10. Bulk and *in situ* jurkat cell CD45 surface marker labeling. (a) Bulk immunostaining of jurkat CD45 cell marker. (b) LCATs *in situ* labeling of jurkat CD45 cell marker. (c) CD45 expression comparison between bulk and LCATs. (N=3). Scale bar: 10 μm.

LCATs in situ surface marker labeling:

To perform *in situ* surface marker staining, 10 μL of 50,000 jurkat cells were first injected into primed LCATs devices. 3 μL of human TruStain FcX (FcRs) were diluted with 20 μL of 1xPBS with 2% FBS and flew through LCATs for 3 mins to block nonspecific binding sites on Fc receptors. After that, 3 μL Alexa Fluor 594-labeled anti-CD45 (Thermo Fisher Scientific, USA) were diluted with 20 μL of 1xPBS and then flew through LCAT for 6 mins. Cells were then washed with 1xPBS with 2% FBS for 6 mins. Cells were then collected from the device and imaged using IX51 Fluorescence Microscopy (Olympus, Japan) and a SLR camera. The images were processed and analyzed using ImageJ.

Table 1. Cell capture efficiency from cell spike-in tests.

	Trial 1	Trial 2	Trial 3
Number of spiked cells	209	94	181
Number of captured cells	194	88	175
Capture Efficiency (%)	92.82	93.62	96.69

Table 2. The number of CTCs and cCAFs collected from breast cancer patients across different stages.

Stage III Patient No.	CTCs	CAFs
1	0	8
2	17	4
3	15	0
4	20	0

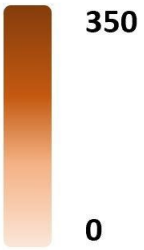

Patient No.	CTCs	CAFs	Stage IV/Metastasis
1*	1	6	Bone
2*	2	NA	Bone, Brain
3*	10	NA	Lung, Bone
4*	11	NA	Bone
5	347	228	Bone, Lung
6	136	264	Bone, Lung
7	52	34	Lung
8	NA	20	NA

*P1 to P4 were processed with blood volumes of 5 mL, 10 mL, 15 mL and 2 mL. The rest of samples were processed with 7.5mL.